Fabrication of Unagglomerated Polypyrrole Nanospheres with Controlled Sizes From a Surfactant-Free Emulsion System

ARTICLE *in* LANGMUIR · SEPTEMBER 2009

Impact Factor: 4.46 · DOI: 10.1021/la9007872 · Source: PubMed

Langmuir
Article
pubs.acs.org/Langmuir

Fabrication of Unagglomerated Polypyrrole Nanospheres with Controlled Sizes From a Surfactant-Free Emulsion System

Sang Won Kim, Hyeon Gu Cho, and Chong Rae Park*

Carbon Nanomaterials Design Laboratory, Global Research Laboratory (GRL), and Department of Materials Science and Engineering, Seoul National University, Seoul 151-744, Republic of Korea

Received March 4, 2009. Revised Manuscript Received April 11, 2009

We developed a very simple, template-free, and environmentally friendly one-step chemical synthesis route to fabricate unagglomerated polypyrrole (PPy) nanospheres. The proposed new fabrication method enables the production of size-controlled unagglomerated PPy nanospheres without the help of any supporting materials such as "hard" and "soft" templates and under mild conditions, viz., room temperature, atmospheric pressure, and no need for acid. From the theoretical calculation, we could find that our novel system was suitable to prepare the unagglomerated PPy spheres. The process is discussed on the basis the classical colloidal and microemulsion theory.

1. Introduction

Nanoparticles of conducting polymers have attracted considerable attention in recent years because of their potential applications in various areas, such as drug deliveries,[1−6] chemical/biosensors,[7−9] encapsulation,[10−12] nanoscale electronics,[13−16] optoelectronics,[17,18] and electrochemical[19−21]and electromechanical devices.[22−25]

Extraordinary physicochemical properties of such conducting polymer nanoparticles can be attributed to high surface area and quantum size effect.[26] Indeed, the electrical, optical, chemical, mechanical, and/or magnetic properties of nanoparticles can be preferentially engineered by controlling their aggregation status, surface structure, and composition, etc.[27,28] However, nanoparticles have an intrinsic tendency to agglomerate due to their increased electrostatic and/or van der Waals interactions arising from the increased surface areas. It has thus been of both theoretical and practical importance and concern to determine how to make unagglomerated conducting polymer nanoparticles with controlled sizes. For example, the applications such as e-papers, electronic devices, and displays require unagglomerated conducting nanoparticles of uniform size.

To satisfy such requirements, two methodologies have been conventionally adopted. One method utilizes "hard" template materials having empty pores such as anodized aluminum oxide (AAO),[29] silicate,[30] and colloidal particles.[26,31] However, the "hard" template methods are complicated, environmentally burdening, and hence expensive processes because the template materials should be removed either by strong acids or bases. Moreover, to control the size of products, various templates with different sizes of inner pores are required. The other methods using "soft" template materials, including surfactant micelles,[32] functionalized organic acids, and polymeric stabilizers,[33] have been successfully applied to the synthesis of unagglomerated conducting polymer nanoparticles with controlled sizes. However, in the "soft" template methods, large quantities of the soft templating materials are often required to control the sizes of nanoparticles. Therefore, the excessive template materials make the processes complex, expensive, and environmentally burdening. It should also be noted that the template materials could never be completely leached out, even by such a heavy removal

*Corresponding author. Tel.: (+82) 2-880-8030; fax: (+82) 2-885-1748; e-mail address: crpark@snu.ac.kr.

(1) Zinger, B.; Miller, L. L. *J. Am. Chem. Soc.* **1984**, *106*, 6861–6863.
(2) Geetha, S.; Rao, C. R. K.; Vijyan, M.; Trivedi, D. C. *Anal. Chim. Acta* **2006**, *568*, 119–125.
(3) Sadki, S.; Schottland, P.; Brodie, N.; Sabouraud, G. *Chem. Soc. Rev.* **2000**, *29*, 283–293.
(4) Ramanavicius, A.; Kausaite, A.; Ramanaviciene, A.; Acaite, J.; Malinauskas, A. *Synth. Met.* **2006**, *156*, 409–413.
(5) Ramanaviciene, A.; Schuhmann, W.; Ramanavicius, A. *Colloids Surf., B* **2006**, *48*, 159–166.
(6) Ramanaviciene, A.; Kausaite, A.; Tautkus, S.; Ramanavicius, A. *J. Pharm. Pharmacol.* **2007**, *59*, 311–315.
(7) Drummond, T. G.; Hill, M. G.; Barton, J. K. *Nat. Biotechnol.* **2003**, *21*, 1192–1199.
(8) Potyrailo, R. A. *Angew. Chem., Int. Ed.* **2006**, *45*, 702–723.
(9) Fu, K. F.; Huang, W. J.; Lin, Y.; Zhang, D. H.; Hanks, T. W.; Rao, A. M.; Sun, Y. P. *Nano Lett.* **2002**, *2*, 311–314.
(10) Marinakos, S. M.; Shultz, D. A.; Feldheim, D. L. *Adv. Mater.* **1999**, *11*, 34–37.
(11) Marinakos, S. M.; Brousseau, L. C.III; Jones, A.; Feldheim, D. L. *Chem. Mater.* **1998**, *10*, 1214–1219.
(12) Martin, C. R.; Parthasarathy, R. V. *Adv. Mater.* **1995**, *7*, 487–488.
(13) Berggren, M.; Nilsson, D.; Robinson, N. D. *Nat. Mater.* **2007**, *6*, 3–5.
(14) MacDiarmid, A. G. *Angew. Chem., Int. Ed.* **2001**, *40*, 2581–2590.
(15) Shirakawa, H.; Louis, E. J.; MacDiarmid, A. G.; Chiang, C. K.; Heeger, A. J. *J. Chem. Soc., Chem. Commun.* **1977**, 578–580.
(16) Greene, R. L.; Street, G. B.; Sutude, L. J. *Phys. Rev. Lett.* **1975**, *34*, 577–579.
(17) Lidzey, D. G.; Bradley, D. D. C.; Alvarado, S. F.; Sedler, D. F. *Nature* **1997**, *386*, 135–136.
(18) Shen, Z.; Burrows, P. E.; Bulovic, V.; Forest, S. R.; Thompson, M. E. *Science* **1997**, *276*, 2009–2011.
(19) Diaz, A. F.; Kanazawa, K. K.; Gardini, G. P. *J. Chem. Soc., Chem. Commun.* **1979**, 635–636.
(20) Saraswathi, R.; Gerard, M.; Malhotra, B. D. *J. Appl. Polym. Sci.* **1999**, *74*, 145–150.
(21) Malinauskas, A.; Malinauskiene, J.; Ramanavicius, A. *Nanotechnology* **2005**, *16*, R51–R62.
(22) Smela, E. *Adv. Mater.* **2003**, *15*, 481–494.
(23) Burroughs, J. H.; Jones, C. A.; Friend, R. H. *Nature* **1988**, *335*, 137–141.
(24) Jager, E. W. H.; Smela, E.; Inganäs, O. *Science* **2000**, *290*, 1540–1545.
(25) Zfar Razzacki, S.; Kthwar, P.; Yang, M.; Mugaz, V.; Burns, M. A. *Adv. Drug Delivery Rev.* **2004**, *56*, 185–198.
(26) Caruso, F.; Caruso, R. A.; Mohwald, H. *Science* **1998**, *282*, 1111–1114.
(27) Mann, S. *Angew. Chem., Int. Ed.* **2000**, *39*, 3392–3406.
(28) Qi, L.; Li, J.; Ma, J. *Adv. Mater.* **2002**, *14*, 300–303.
(29) Martin, C. R. *Science* **1994**, *266*, 1961–1966.
(30) Wu, C. G.; Bein, T. *Science* **1994**, *264*, 1757–1759.
(31) Marinakos, S. M.; Novak, J. P.; Brousseau, L. C.III; House, A. B.; Edeki, E. M.; Feldhaus, J. C.; Feldheim, D. L. *J. Am. Chem. Soc.* **1999**, *121*, 8518–8522.
(32) Jang, J.; Oh, J. H.; Stucky, G. *Angew. Chem., Int. Ed.* **2002**, *41*, 4016–4019.
(33) Armes, S. P.; Vincent, B. *J. Chem. Soc., Chem. Commun.* **1987**, 288–290.

process, and the residual template materials tend to lower the electrical conductivity of conducting materials.

During the past decades, a couple of groups have reported on surfactant-free emulsion systems: (i) the colloidal stabilization of oil-in-water (o/w) emulsions with the addition of hydrophobic polymers into oil droplets,[34] (ii) the colloidal stabilization of o/w emulsions with sequential megasonic irradiation,[35] (iii) particle-stabilized surfactant-free emulsion and their use for material fabrication,[36] and (iv) surfactant-free emulsions of water and near- and supercritical carbon dioxide ($ssCO_2$).[37] However, most of papers have focused on the methodology for surfactant-free o/w preparation, and only a few represent the utilization of them for nanomaterials fabrication. This is because the earlier reported systems can make stable emulsions but require some special equipment and/or supporting materials such as hydrophobic polymers, sequential megasonic irradiation, certain solid nanoparticles as stabilizing agents, and $ssCO_2$. On the other hand, "surfactant-free emulsion" was recently introduced whereby the stability of emulsions was achieved by removing dissolved gases in an emulsion system with degassing[38,39] and/or freeze−thaw[40] methods. Basically, the dissolved gases in o/w emulsions contribute to strengthening the hydrophobic attraction of the droplets, hence disturbing the emulsion stability. If the dissolved gases are removed from the emulsion system, the emulsion stability can then be consequently achieved. However, this kind of emulsion was observed only in the emulsion system consisting of long-chain alkane (*n*-dodecane) and water. Moreover, there have been some reports negating the emulsion-stabilization effect by the removal of the dissolved gases.

Herein we report maybe the first practical utilization of the "surfactant-free emulsion" system as a nanoreactor to fabricate unagglomerated polypyrrole (PPy) nanospheres. This new approach is a very easy and environmentally friendly one-pot synthesis pathway, characterized by its mild reaction conditions (room temperature, ambient pressure), very short reaction time (within 10 min), and no need for any supporting materials such as surfactants or hard templates. In addition, this newly proposed method makes it possible to fabricate very pure and unagglomerated PPy nanoparticles of controlled sizes. Typical unagglomerated PPy nanospheres could be obtained by polymerizing pyrrole monomers in a surfactant-free water/octanol microemulsion system. The results could be well supported with the fundamental principles for a microemulsion system.

2. Theoretical Considerations on Surfactant-Free Water/Oil Emulsion System

2.1. Stability of Water Droplets. The theories for colloidal and microemulsion systems describe the stability of water droplets in terms of the surface energy (G) as given in eq 1.[41]

$$G = \frac{3}{R_d} V_d f_s \quad (1)$$

Here, R_d is the radius of water droplets, V_d is the total volume of water, and f_s is the interfacial tension between water and organic solvent.

This equation describes that, with a given amount of water and the assumption that the size of water droplets formed by a sonication is independent of the kinds of organic solvents in continuous phase, the total surface energy of water droplets is determined solely by the interfacial tension at the interface between water droplets and a solvent. The surface energy values for the solvents used in this study can then be calculated as listed in Table 1. Here, the literature value of f_s was used for the calculation, and the diffusion coefficient (D) of water droplets was also calculated using the literature value of viscosity (η) of the solvents for the later discussions. It can be clearly seen that the G value itself is 5 times lower in ethyl acetate and 4 times lower in octanol than that in benzene. That is, the water droplets formed in ethyl acetate and octanol are more resistant to the coalescence than those in benzene.

However, since the water droplets can be coalesced by aggregation or collision on Brownian motion in the continuous phase, the kinetic aspect of water droplets should also be considered to see whether the water droplets are to agglomerate.

2.2. Diffusion of Water Droplets. To consider the mobility of water droplets in the continuous phase, the diffusion coefficient of water droplets in a specified continuous phase was calculated and shown in Table 1. In general, the Stokes−Einstein relation (eq 2) describes the dependence of the diffusion coefficient (D) of a water droplet[42] on the viscosity of a continuous phase and the temperature of a system:

$$D = \frac{k_B T}{6\pi\eta R_d} \quad (2)$$

where k_B is the Boltzmann constant, T is the absolute temperature, and η is the viscosity of the continuous phase.

At a given temperature, the diffusion coefficient of the water droplets is inversely proportional to the viscosity of the continuous phase. This implies that the lower the viscosity of the continuous phase, the higher the mobility of water droplets and, as a consequence, the higher the tendency of coalescence of the water droplets.[28,43] When considered with the values of G and D in Table 1, we can immediately learn that the stability of water droplets in each continuous phase is in the order of octanol, ethyl acetate, and benzene. We can therefore predict that the water droplets in the octanol phase can play the role of nanoreactors by providing stable interfaces for an interfacial polymerization of pyrrole monomers.

In recent work, Tieleman et al. reported from the molecular dynamics computer simulations of 1-octanol and its mixtures with water[44] that, upon the addition of water, the clusters composed of hydrocarbons and hydroxyl groups become spherical, whereby the polar regions enriched in hydroxyl groups of octanol and water and nonpolar regions enriched in hydrocarbon tails of octanol coexist. These polar regions surrounded by hydrocarbon tails have led to the formation of "inverted micelles".

3. Experimental Details

3.1. Materials. Benzene (>99% purity, Fluka), ethyl acetate (>99.5% purity, Aldrich), 1-octanol (>99% purity, Aldrich) and

(34) Kamogawa, K.; Kuwayama, N.; Katagiti, T.; Akatsuka, H.; Sakai, T.; Sakai, H.; Abe, M. *Langmuir* **2003**, *19*, 4063–4069.
(35) Kamogawa, K.; Okudaira, G.; Matsumoto, M.; Sakai, T.; Sakai, H.; Abe, M. *Langmuir* **2004**, *20*, 2043–2047.
(36) Binks, B. P.; Murakami, R. *Nat. Mater.* **2006**, *5*, 865–869.
(37) Timko, M. T.; Diffendal, J. M.; Tester, J. W.; Smith, K. A.; Peters, W. A.; Danheiser, R. L.; Steinfeld, J. I. *J. Phys. Chem. A* **2003**, *107*, 5503–5507.
(38) Pashley, R. M. *J. Phys. Chem. B* **2003**, *107*, 1714–1720.
(39) Maeda, N.; Rosenberg, K. J.; Israelachvili, J. N.; Pashley, R. M. *Langmuir* **2004**, *20*, 3129–3137.
(40) Burnett, G. R.; Atkin, R.; Hicks, S.; Eastoe, J. *Langmuir* **2004**, *20*, 5673–5678.
(41) Ruckenstein, E.; Chi, J. C. *Faraday Trans. 2* **1975**, *71*, 1690–1707.
(42) Aveyard, R.; Binks, B. P.; Esquena, J. P.; Fletcher, D. I.; Buscall, R.; Davis, S. *Langmuir* **1999**, *15*, 970–980.
(43) Holmberg, K.; Jönsson, B.; Kronberg, B.; Lindman, B. *Surfactants and Polymers in Aqueous Solution*, 2nd ed.; Wiley: New York, 2002; Chapter 21.
(44) MacCallum, J. L.; Tieleman, D. P. *J. Am. Chem. Soc.* **2002**, *124*, 15085–15093.

Table 1. The Calculated Values of Surface Energy (G) and Diffusion Coefficient (D) of Water Droplets in Organic Solvents Together with the Interfacial Tension (f_s) and Viscosity (η) of the Solvents Used in This Study

		Organic solvents		
		benzene	ethyl acetate	octanol
literature value	f_s[a] (mNm^{-1})	34.1	6.8	8.5
	η[b] (cP)	0.601	0.419	7.182
calculated value	G[c] (10^{-9} J R_d^{-1})	102.3	20.4	25.5
	D[d] (10^{-22} m^2 s^{-1} R_d^{-1})	3.63	5.21	0.303

[a] Literature value of interfacial tension with water (*from the CRC Handbook of Chemistry and Physics*). [b] Viscosity of solvent (*from the CRC Handbook of Chemistry and Physics*). [c] Calculated surface energy of water droplets. [d] Calculated diffusion coefficient of water droplets.

distilled and deionized water were used as solvents in our system. Pyrrole (98% purity, Aldrich) was purified by distillation under reduced pressure. Ferric chloride ($FeCl_3$) (98% purity, Aldrich) was used as an oxidant without further treatment. Ultrasonic irradiation was performed for the emulsification of water droplets in the various organic solvents. The ultrasound was accomplished with a high-intensity ultrasonic probe (SONOPULS HD2200, BANDELIN, Germany, 1 cm diameter Ti horn, 20 kHz, 50 Wcm^{-2}).

3.2. Preparation Method. *Formation of Water Droplets in Octanol.* To verify the theoretical consideration that stable droplets could be formed in a water-in-octanol system, the several experiments were carried out by using the mixed solvents with water and octanol. The volume ratio of water to octanol was varied in the range of 1/10, 1/20, 1/40, and 1/80 (denoted WO110, WO120, WO140, and WO180, respectively). An ultrasound was used to irradiate the mixed solutions for 1 min. After the sonication, the dispersion state was monitored. In the case of WO110 and WO120 samples, the translucent solution was separated into two phases of water and octanol within 1 min after the sonication. For WO140 and WO180 samples, the mixed solutions became transparent by the sonication, and the phase separation was not observed for up to 12 h after. From these observations, we expected that stable water-in-oil emulsions would be formed in the WO140 and WO180 samples. The sizes of water droplets in the samples were investigated by dynamic light scattering (DLS).

Fabrication of PPy Spheres. In a typical synthesis, ferric chloride ($FeCl_3$) dissolved in distilled water of 1 mL was admixed with octanol of 40 mL, and then sonicated for 1 min with an ultrasonic homogenizer. Pyrrole monomer was added to the mixture under sonication for an additional minute. The color of the solution turns from pale yellow to black within 5 min. After a specified time in the range of 5 to 10 min, an excess amount of methanol and distilled water were poured into the system to get the precipitates of PPy. The precipitates were then filtered, washed with methanol and distilled water to remove unreacted monomers and oxidants, and finally vacuum-dried at 50 °C for 24 h. For the comparative experiments, the continuous phase was changed from octanol to water, benzene, and ethyl acetate, and other conditions were kept the same.

3.3. Characterization. *Dynamic Light Scattering.* Measurement of droplet size distribution was performed by DLS with DLS-7000 (Otsuka Electronics Co., Japan) employing a 75 mW Ar laser (λ = 488 nm) at 25 °C. The CONTIN algorithm was used to determine an intensity-weighted average hydrodynamic radius of the droplets. The parameters (density, viscosity, and refractive index) of the dispersant (water droplets) and dispersed medium (octanol) were calculated on the basis of known literature values.

Microscopy. The morphologies of PPy were examined using field emission scanning electron microscopy (FESEM, JEOL JSM-6330F) and transmission electron microscopy (TEM, Philips TECNAI F20). For FESEM measurement, the washed and vacuum oven-dried PPy powders were scattered on adhesive carbon tapes, which were then mounted on copper microstubs. The powders were platinum-sputter-coated for 2 min using a sputter coater (JFC-1100, JEOL, Japan). TEM samples were prepared by drying drops of dilute dispersion on copper grids.

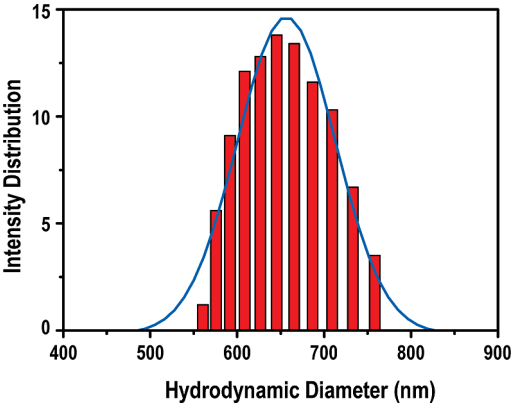

Figure 1. The size distribution of reverse micelle droplets in the system of water/octanol = 1:40 v/v, determined by DLS, shows Gaussian distribution.

4. Results and Discussion

4.1. Formation of Water Droplets. The size of water droplets of the WO140 sample could be determined using the DLS measurement, as shown in Figure 1 (Unfortunately, in the case of the WO180 sample, the concentration of water is too dilute to measure the size using DLS). It can be seen that the WO140 water-in-octanol system produces stable spherical and monodispersed droplets with hydrodynamic diameter of 650 nm. The droplet size was sustained for up to 12 h. This result experimentally confirms the formation of stable reversed micelle droplets as predicted by Tieleman et al.'s computational simulation. So, these reversed micelle droplets could be utilized as a nanoreactor for the formation of unagglomerated PPy nanoparticles.

4.2. Formation of Unagglomerated PPy Spheres. Indeed, Figure 2a clearly shows that the unagglomerated spheres of PPy with an average diameter of 600 nm were successfully fabricated in the reversed micelle droplets, without using any supporting materials such as templates and surfactants. Indeed, when redispersed in methanol solution, the obtained PPy particles were homogeneously dispersed with a simple magnetic stirring, confirming the successful synthesis of unagglomerated PPy nanoparticles. The observed diameter of PPy spheres is in good agreement with the hydrodynamic diameter of water droplets determined using DLS measurement. It is interesting to note in Figure 2b that each large particle of 600 nm in mean diameter consists of the nanoparticles with a diameter below 40 nm (white arrows). A TEM image (Figure 2c) also confirms this morphology. From these figures, we can conjecture the formation mechanism of the unagglomerated larger particles as shown in Figure 3.

In the experiment, the ultrasound pulse was applied periodically, i.e., pulse (T_{ON}) and rest (T_{OFF}) periods, as shown in Figure 3. During the T_{ON} period, water droplets are formed in the continuous phase of octanol to form a transparent water-in-oil emulsion (step 1). Since the T_{ON} and T_{OFF} periods are alternating, water droplets get bigger by the coalescence during the T_{OFF} periods. Because the breakage of droplets generally happens in a very short time (~1 μs) compared to the growth of droplets (~10 μs),[45] the size of dispersed water droplets decreases

(45) Grieser, F.; Ashokkumar, M. *Colloids and Colloid Assemblies*; Caruso, F., Ed.; Wiley: Weinheim, Germany, 2004; Chapter 4.

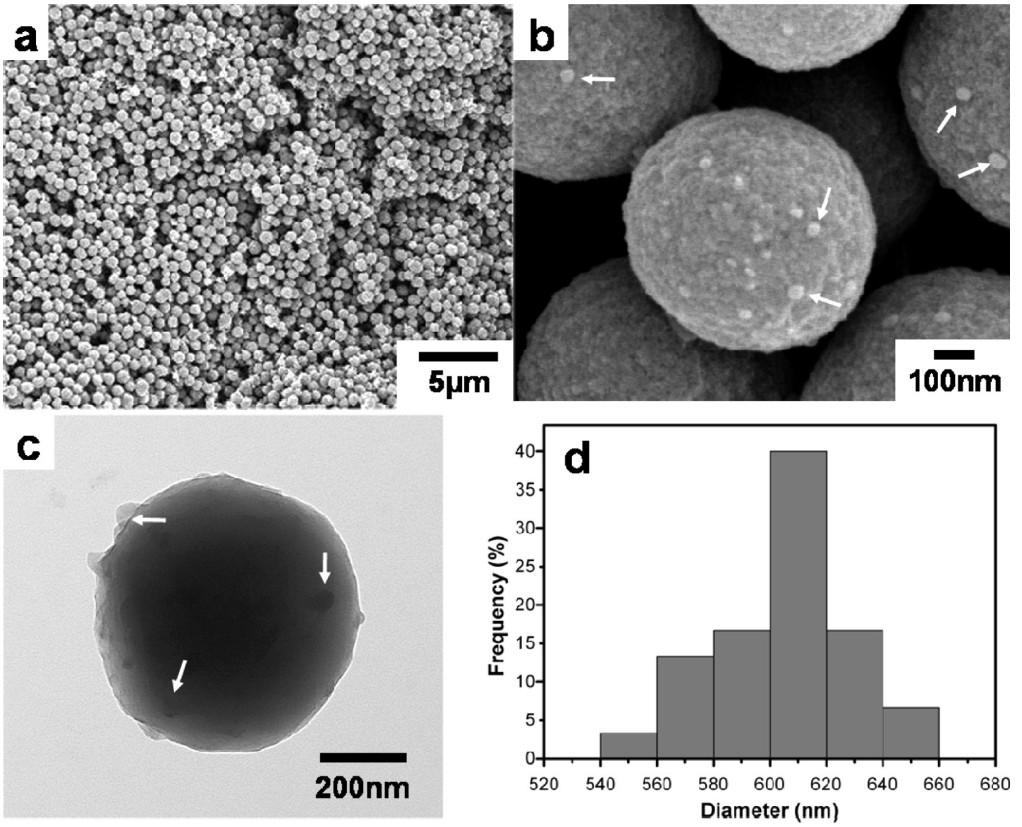

Figure 2. (a) Low-magnification and (b) high-magnification SEM images of the as-synthesized PPy spheres. (c) TEM image of a PPy sphere and (d) statistical size distribution of the spheres.

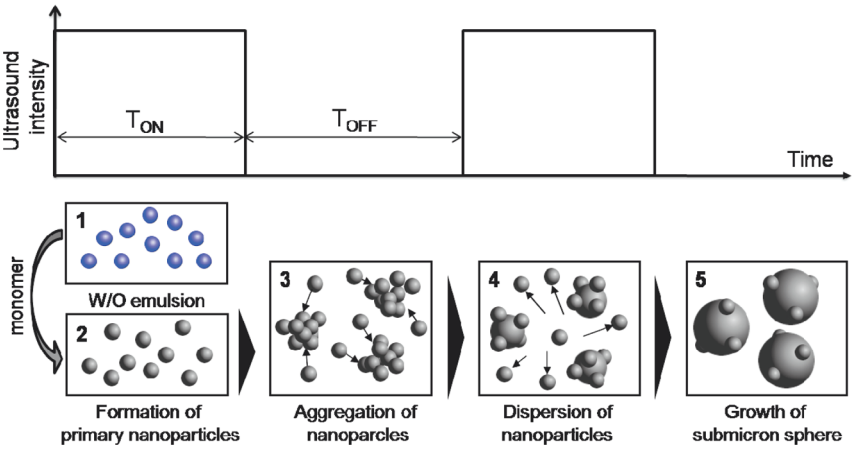

Figure 3. Schematic representation of the ultrasound pulse cycles and the formation mechanism of the unagglomerated PPy spheres in the reversed micelle droplets formed in water-in-octanol (W/O) system under a periodic ultrasound irradiation.

toward a minimum critical size under the periodic ultrasonic field. The minimum critical size of droplets is determined by several parameters such as ultrasound frequency, viscosity of the medium, etc., which are also affected on the maximum critical size of droplets during the T_{OFF} period. When pyrrole monomers are introduced into the solution (step 1→2), the polymerization reaction starts only at the interface of water droplets because the oxidant, $FeCl_3$, cannot diffuse out of the water droplets to the octanol phase. But, since the oxidized pyrrole monomers and the growing oligomers can diffuse into the water droplets due to their hydrophilicity, primary nanoparticles below 40 nm in diameter are formed within the water droplets (step 2). Such primary nanoparticles, a kind of building block, are then self-assembled into the larger particles so as to lower their surface energies during the T_{OFF} period (step 3). The polymeric primary nanoparticles keep growing during the T_{OFF} period because of the reaction between the propagating radical species on the surface of the particles. However, the growth of the particles would be governed by both the diffusion rate of the primary nanoparticles to the growing particles and the number of primary nanoparticles around the growing particles. Since these two factors are strongly influenced by the alternating T_{ON} and T_{OFF} periods (step 4), the size of the finally obtained particles is determined by the rate ratio of diffusion-to to diffusion-out of the primary particles and the radical lifetime on the surface of the growing particle surface (step 5).

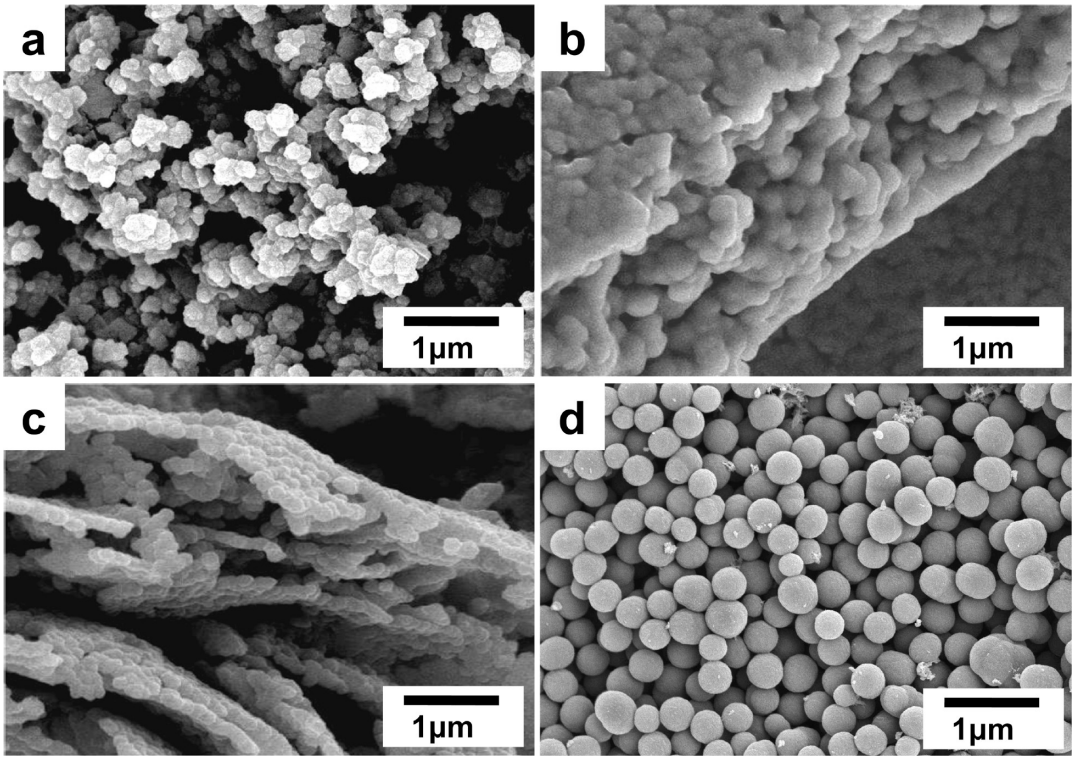

Figure 4. SEM images of PPy synthesized by a novel method using various solvents as a continuous phase: (a) water, (b) benzene, (c) ethyl acetate, and (d) octanol.

From a series of additional experiments using various solvents, such as water, benzene, and ethyl acetate, we found octanol to be one of the most suitable organic solvent as a continuous phase in this kind of reaction system (see Figure 4).

As shown in Figure 4a, when water is the continuous phase in the synthesis of PPy particles, we could not obtain unagglomerated nanoparticles, but rather all agglomerated particles with a cauliflower-like morphology, typical of bulk and/or solution-polymerized PPy. As for benzene and ethyl acetate, the primary nanoparticles tended to self-assemble into pancake-like and sheet-like morphologies, respectively.

However, when the polymerization of pyrrole was carried out in octanol, unagglomerated particles with a spherical morphology were exclusively obtained.

To find the reasons of the unagglomeration of obtained particles, we analyzed our reaction system in terms of the stability of PPy particles.

4.3. Stability of PPy Particles. The agglomeration of PPy particles can occur by sedimentation due to the gravity effect. It is therefore necessary to consider the effect of sedimentation on the stability of PPy particles.

The measurement of the size of PPy particles from SEM images enabled us to estimate the sedimentation rate (V_s) of PPy particles using Stokes' law,[42,46] as shown in eq 3.

$$V_s = \frac{2}{9}\frac{R^2 g \Delta\rho}{\eta} \tag{3}$$

where R is the radius of particles, g is the gravity, $\Delta\rho$ is the density difference of particles and medium, and η is the viscosity of medium. A calculated sedimentation rate by using the average size (R = 300 nm; counted 100 spheres) of PPy particles was 1.76×10^{-8} ms^{-1}. In a general colloidal system, if the sedimentation rate is higher than 4.4×10^{-5} ms^{-1}, the colloid will precipitate as a result of the gravity.[43,46] The sedimentation time determined by using the height of a reaction vessel (4.5 cm) is about 30 days, which is the time required for the complete sedimentation of PPy spheres from the top position in the reaction solution. If the PPy spheres were well-distributed in the solution, their average sedimentation rate would be 15 days. This result indicates that all the PPy spheres in octanol were kinetically very stable, and, as a consequence, they could be obtained as unagglomerated. In contrast, in the cases of benzene and ethyl acetate, the water droplets were unstable in a continuous phase so that they could not maintain their spherical shapes as a result of the high surface energy. So, the water droplets tended to aggregate to reduce their surface area, and hence the phase separation occurred to form the upper organic solvent and lower aqueous layers. As the polymerization of pyrrole took place at the interface between organic solvent and water layers, and the sedimentation of PPy particles was accelerated because of the aggregated water droplets, a film or sheet-like morphology of PPy particles could be observed as shown in Figure 4b,c.

4.4. Size Control of Unagglomerated PPy Spheres. On the basis of our proposed formation mechanism for the unagglomerated PPy spheres, it may possibly be expected to control the size of PPy spheres by changing the collision rate of the building-block-like nanoparticles approximately 40 nm in size. Indeed, a general collision theory tells that a collision rate is proportional to the collision frequency (Z) as defined in eq 4.

$$Z = \sigma \bar{c}_{rel} \frac{N}{V_c} \tag{4}$$

where σ is the collision cross-section ($= \pi R^2$), c_{rel} is the relative mean speed, N is the number of particles, and V_c is the total

(46) Reddy, S. R.; Melik, D. H.; Fogler, H. S. *J. Colloid Interface Sci.* **1981**, *82*, 116–127.

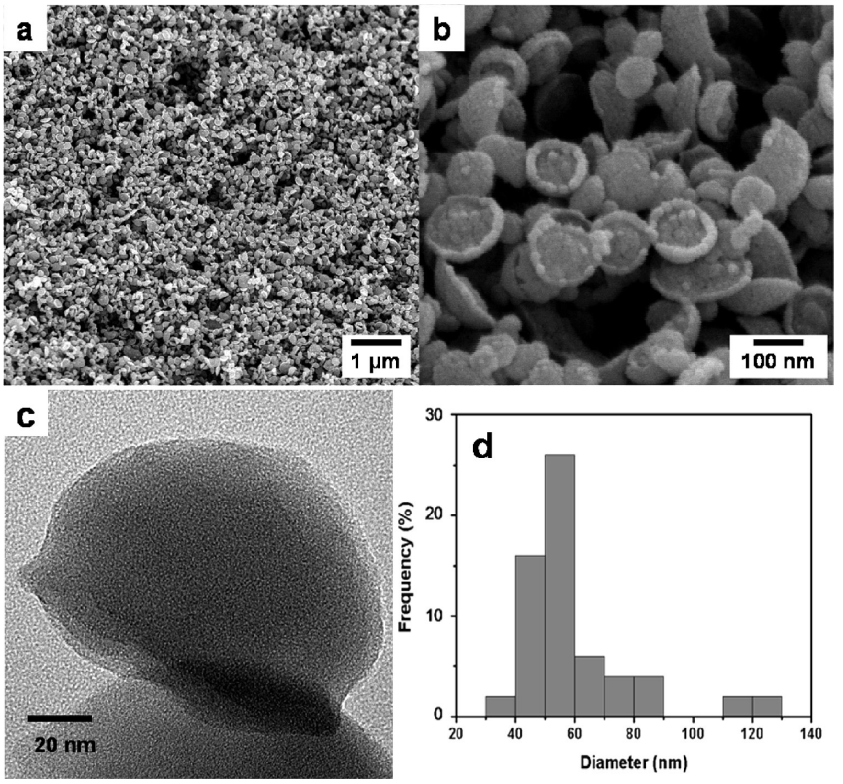

Figure 5. (a) Low-magnification and (b) high-magnification SEM images and (c) TEM image of PPy "flying disk-like" spheres as synthesized at a water/octanol volume ratio of 1/80. (d) Statistical size distribution of spheres.

volume of continuous phase. As $\sigma = \pi R^2$ and $N = V_p/[(4/3)\pi R^3]$, then $Z = (3/4R)(V_p/V_c)\bar{c}_{rel}$, where V_p is the total volume of particles.

Since the relative mean speed of the building block nanoparticles in the same continuous phase can be assumed to be constant, the collision frequency of the building block nanoparticles is proportional to a volume ratio of the total dispersed particles and the continuous medium. In our experimental scheme, the volume ratio of the aqueous solution to the octanol therefore appears to be a key factor that determines the collision frequency of building block nanoparticles and the final size of PPy spheres. To examine this assumption, we changed the volume ratio of water to octanol from 1/40 to 1/80, and indeed confirmed that the average size of PPy particles is reduced to about 60 nm (Figure 5). It is, however, interesting to note that the morphology of the particles changes somehow to a shell-like or "flying disk" morphology as shown in Figure 5b, c. This result implies that the diameter of PPy particles itself is controlled by the volume ratio of water and octanol, but the morphology of the particles can also be influenced. Indeed, we can note that the surface free energy of PPy particles increases as much as about 100 times concurrently with the decrease in the diameters of PPy particles from approximately 600 to 60 nm. Such high surface free energy of PPy particles is likely to contribute to forming rather "flying disk" morphology of the particles through a fusion and aggregation of the PPy particles. Interfacial assembly of nanoparticles is dictated by a minimization of the Helmholts free energy.[47] Placement of one nanoparticle at an interface will decrease the entropy by about k_B (the Boltzmann constant). Consequently, the energy change, ΔE , must be negative to reduce the total energy. The three contributions to the interfacial energy arise from the interfacial tensions between the three components ($f_{P/O}$: particle−oil; $f_{P/W}$: particle−water; $f_{O/W}$: oil−water). ΔE, as a result of the assembly of a single particle at the oil−water interface, is given by eq 5:[48,49]

$$\Delta E = -\frac{\pi R^2}{f_{O/W}}[f_{O/W} - (f_{P/W} - f_{P/O})]^2 \quad (5)$$

Because ΔE depends on R^2, the energy gain is smaller, and the assembly is less stable for smaller nanoparticles than for larger ones. Therefore, less-stable assembly behavior may have led to different types of morphologies. However, the exact formation mechanism of such "flying disk" morphology needs a systematic detailed study. One promising implication of this result is the possibility of morphology control of the PPy particles by a very simple treatment, which will be our future work.

5. Conclusions

In conclusion, the unagglomerated PPy spheres can be successfully prepared by a simple and environmentally friendly method in a short time without using hard and/or soft templates. The formation mechanism of PPy spheres was well correlated to the colloidal and emulsion theories. From the theoretical calculation, we could find that our novel system was suitable to prepare unagglomerated PPy spheres. By simply changing the water-to-octanol volume ratio, we could obtain smaller spheres with controllable sizes. Our novel approach demonstrated the first experimental evidence for the formation of reversed micelle

(47) Lin, Y.; Skaff, H.; Emrick, T.; Dinsmore, A. D.; Russell, T. P. *Science* **2003**, *299*, 226–229.

(48) Pieranski, P. *Phys. Rev. Lett.* **1980**, *45*, 569–572.
(49) Binks, B. P.; Clint, J. H. *Langmuir* **2002**, *18*, 1270–1273.

droplets from a simple mixing of two liquids, viz., water and octanol in our case, which will then be utilized for the fabrication of unagglomerated polymer spheres with controllable sizes using only pure solvents in the absence of templates or surfactants.

Acknowledgment. This work was supported by the Korea Foundation for International Cooperation of Science & Technology (KICOS) through a grant provided by the Korean Ministry of Education, Science & Technology (MEST) (K20704000008).